Infinite Science
Publishing

Proceedings Article

A Deep Learning Approach for Automatic Image Reconstruction in MPI

Tobias Knopp [1,2,*]· Paul Jürß [1,2]· Mirco Grosser [1,2]

[1]Section for Biomedical Imaging, University Medical Center Hamburg-Eppendorf, Hamburg, Germany
[2]Institute for Biomedical Imaging, Hamburg University of Technology, Hamburg, Germany
*Corresponding author, email: t.knopp@uke.de

Abstract
Image reconstruction in magnetic particle imaging is a challenging task because the optimal image quality can only be obtained by tuning the reconstruction parameters for each measurement individually. In particular, it requires a proper selection of the Tikhonov regularization parameter. In this work we propose a deep-learning-based post-processing technique, which removes the need for manual parameter optimization. The proposed neural network takes several images reconstructed with different parameters as input and combines them into a single high-quality image.

I. Introduction

Determining the particle concentration in magnetic particle imaging (MPI) requires the solution of an ill-posed inverse problem. A stable solution can only be achieved by applying some type of regularization [1]. The most common method addresses this issue by the use of Tikhonov regularization. A drawback is that it requires proper selection of the regularization parameter to find a good compromise between noise reduction and loss of spatial resolution. In MPI, this is often done manually, which is time consuming, does not guarantee an optimal solution, and depends on the observer.

The goal of this paper is to develop an automatic reconstruction pipeline using deep learning (DL). DL can be applied for image reconstruction in several ways. It can be used to learn the inverse imaging operator [2, 3], but this requires a large amount of training data and ignores any knowledge about the imaging process that can help building the model. Another option is to use a neural network only for regularization, as has been done recently in the context of MPI by integrating a learned denoiser into the ADMM reconstruction algorithm [4]. A neural network is also used for regularization in the Deep Image Prior, which was studied for MPI in [5, 6].

II. Methods and Materials

In MPI, the relation between the discrete measurement $\boldsymbol{u} \in \mathbb{C}^M$ and the unknown particle concentration vector $\boldsymbol{c} \in \mathbb{C}^N$ is linear and can be expressed as

$$\boldsymbol{S}\boldsymbol{c} + \boldsymbol{\varepsilon} = \boldsymbol{u} \tag{1}$$

where $\boldsymbol{S} \in \mathbb{C}^{M \times N}$ is the system matrix describing the physics of an MPI experiment and $\boldsymbol{\varepsilon} \in \mathbb{C}^M$ is statistical noise that is added during the measurement process.

Image reconstruction in MPI involves computing $\boldsymbol{c}$ by solving the inverse problem (1) using an appropriate method that prevents noise amplification. One common approach is to solve the regularized least-squares problem

$$\boldsymbol{c}_\lambda = \psi_{\boldsymbol{S},\lambda}(\boldsymbol{u}) := \operatorname*{argmin}_{\boldsymbol{c}} \|\boldsymbol{S}\boldsymbol{c} - \boldsymbol{u}\|_2^2 + \lambda\|\boldsymbol{c}\|_2^2, \tag{2}$$

where λ is a regularization parameter that allows to balance between noise and spatial resolution of the solution $\boldsymbol{c}_\lambda$. High noise requires larger λ and reduces the spatial resolution. Low noise allows to reduce λ and get better spatial resolution. Computationally, we consider $\psi_{\boldsymbol{S},\lambda} : \mathbb{C}^M \to \mathbb{R}^N$ to be a cheap reconstruction method since it can be solved efficiently with only $\mathcal{O}(MN)$ operations using few Kaczmarz iterations [7].
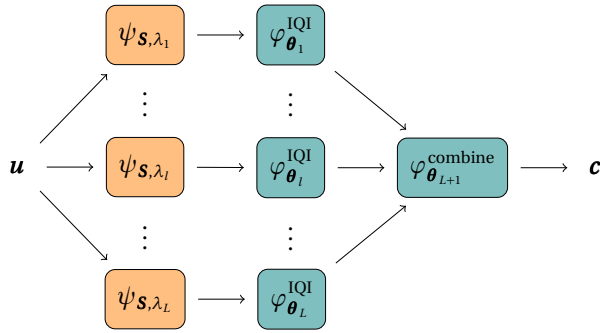
Figure 1: Overview of the proposed image reconstruction pipeline.

II.I. Proposed Method

Our approach is based on performing L pre-processing reconstructions with decreasing regularization parameters λ_l, $l = 1,\ldots,L$, of which we know that one will roughly correspond to the optimal λ. The resulting c_{λ_l}, $l = 1,\ldots,L$, can thus be viewed as a multi-channel reconstruction. There are now three tasks to be addressed in order to end up with a single high quality reconstruction:

1. noisy channels need to be denoised

2. blurry channels need to be improved in resolution

3. all channels need to be combined

The first two steps can be combined under the term *image quality improvement* (IQI) and are tasks, for which deep neural networks (DNNs) perform exceptionally well. We thus introduce a DNN $\varphi_{\boldsymbol{\theta}_l}^{\mathrm{IQI}} : \mathbb{R}^N \to \mathbb{R}^N$, which has the same architecture but different network parameters $\boldsymbol{\theta}_l$ for each channel. After the initial pre-reconstruction, the image quality is improved by applying $\varphi_{\boldsymbol{\theta}}^{\mathrm{IQI}}$, i.e., we calculate

$$\omega_{\boldsymbol{S},\lambda_l,\boldsymbol{\theta}_l}^{\mathrm{IQI}}(\boldsymbol{u}) = \varphi_{\boldsymbol{\theta}_l}^{\mathrm{IQI}}\left(\frac{1}{\alpha}\psi_{\boldsymbol{S},\lambda_l}(\boldsymbol{u})\right), \quad l = 1,\ldots,L, \quad (3)$$

where $\alpha = \|\psi_{\boldsymbol{S},\lambda_1}(\boldsymbol{u})\|_\infty$ is a normalization factor. Note that α is computed with respect to the first channel, because the latter is the most robust to noise due to its large regularization parameter. Finally, we need to combine all channels into a single one, which can be done by another DNN $\varphi_{\boldsymbol{\theta}_{L+1}}^{\mathrm{combine}} : \mathbb{R}^{N\times L} \to \mathbb{R}^N$. The proposed reconstruction method, which we name MPIPostProcNet, is obtained by combining all sub-networks as outlined in Figure 1. Mathematically, the reconstruction pipeline can thus be written as

$$\omega_{\boldsymbol{S},\boldsymbol{\lambda},\bar{\boldsymbol{\theta}}}^{\mathrm{reco}}(\boldsymbol{u}) = \alpha\varphi_{\boldsymbol{\theta}_{L+1}}^{\mathrm{combine}}\left(\omega_{\boldsymbol{S},\lambda_1,\boldsymbol{\theta}_1}^{\mathrm{IQI}}(\boldsymbol{u}),\ldots,\omega_{\boldsymbol{S},\lambda_L,\boldsymbol{\theta}_L}^{\mathrm{IQI}}(\boldsymbol{u})\right), \quad (4)$$

where we grouped all the training parameters $\boldsymbol{\theta}_l$ into a single vector $\bar{\boldsymbol{\theta}}$ and the regularization parameters into $\boldsymbol{\lambda} = (\lambda_l)_{l=1}^L$.

II.II. Training

The parameters of the neural network are trained in an end-to-end fashion using J training pairs $(\boldsymbol{u}_j, \boldsymbol{c}_j)$, $j = 1,\ldots,J$. Training is performed by solving the minimization problem

$$\sum_{j=1}^J D(\omega_{\boldsymbol{S},\boldsymbol{\lambda},\bar{\boldsymbol{\theta}}}^{\mathrm{reco}}(\boldsymbol{u}_j), \boldsymbol{c}_j) \xrightarrow{\bar{\boldsymbol{\theta}}} \min \quad (5)$$

where D is a distance measure for which we use the normalized root mean square deviation (NRMSD). Eq. (5) is optimized using Adam with default momentum settings of $\beta = (0.9, 0.999)$, a learning rate of $\eta = 10^{-3}$, a batch size of four and 100 epochs.

Training data is synthesized using a hybrid approach. We generate random images $\boldsymbol{c}_j$ using ellipsoids that are randomly scaled, rotated and convolved with a randomly chosen Gaussian kernel. Then, the MPI measurement data is generated by calculating $\boldsymbol{u}_j = \boldsymbol{S}\boldsymbol{c}_j + \boldsymbol{\varepsilon}_j$ where $\boldsymbol{S}$ is a measured MPI system matrix and $\boldsymbol{\varepsilon}_j \sim \mathcal{N}(0, \sigma^2)$ is white Gaussian noise whose variance σ^2 is derived from measurements that are acquired when measuring $\boldsymbol{S}$. The maximum concentration of $\boldsymbol{c}_j$ is scaled such that the resulting SNR fits into one of the noise classes $\mathrm{SNR}_p = \left[5 + 2.3^{p-1}, 5 + 2.3^p\right)$, $p = 1,\ldots,P$ with $P = 7$ leading to a dynamic range of about 340. The regularization parameter is chosen as $\lambda_l = \left(\frac{1}{50}\right)^{l-1}$, $l = 1,\ldots,L$ with $L = 4$. For $\psi_{\boldsymbol{S},\lambda}$ 10 Kaczmarz iterations were used. In total we used $J = 500$ images for training and 140 images for testing. In addition to the synthesized test data we apply the method to the experimental data from the OpenMPI-Data set [8]. A matching 3D system matrix with the same 3D Lissajous sequence as used for the OpenMPIData but with a higher resolution of $22 \times 22 \times 24$ is used in all experiments.

For the denoising network, we use a U-Net like encoder-decoder architecture [9]. In the encoder part, downsampling was implemented using max pooling layers whereas the upsampling in the decoder was performed using fixed trilinear upsampling filters. The leaky ReLu activation function was used throughout the denoising network. In addition to the regular concatenating skip-connections, we added a residual connection connecting the network input to its output, as was done in [10]. Thus, the U-Net itself effectively learns the difference between the pre-reconstruction and the improved image estimates. For the combination network, we use a single convolutional layer followed by an Gaussian error linear unit activation function. All convolutional layers apply kernels of size $(3, 3, 3)$.
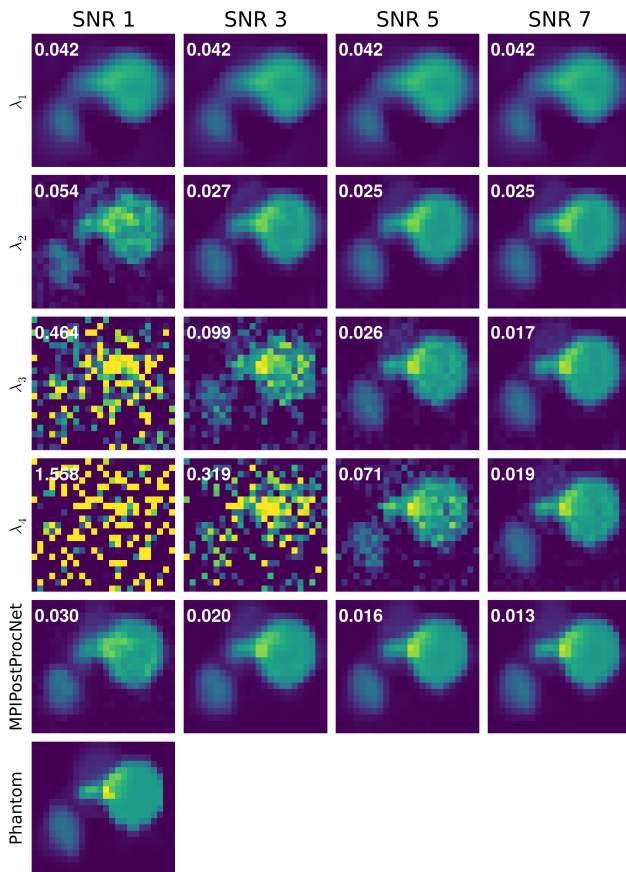
Figure 2: Example results for one of the test datasets (13th xz slice). Columns show the results for different SNR classes. The first four row show the pre-reconstructions $\psi_{S,\lambda}(\boldsymbol{u}^{\text{test}})$ for different regularization parameters λ. The fifth row shows the result after application of the neural network postprocessing $\omega_{S,\lambda,\hat{\theta}}^{\text{reco}}(\boldsymbol{u}^{\text{test}})$. The ground truth $\boldsymbol{c}^{\text{test}}$ is show in the last row. The NRMSD is displayed in the upper left part of each reconstruction.

III. Results

Reconstruction results for an example test dataset are shown in Figure 2. One can see that the best image for the pre-reconstructions depends on the chosen λ when changing the SNR class. For instance, the first SNR class requires a very high regularization parameter λ_1 while the optimal regularization parameter for SNR class 3 is λ_2 and for SNR class 7 is λ_4. In comparison, the neural network always yields the best image quality.

A quantitative analysis of all test data is outlined in Figure 3. Shown are box plots for all pre- and post-processing reconstruction methods and all considered SNR classes. One can see that the best pre-reconstructions indeed depend on the considered noise level. In ocher color, the statistics is summarized by always taking the best reconstruction from all pre-reconstructions based on the NRMSD. This can be considered to be an idealized case since a practice, no ground
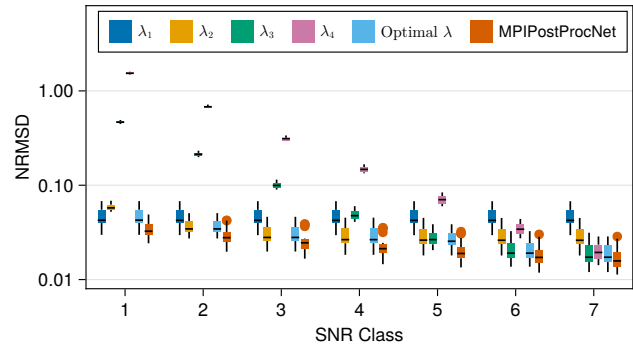

Figure 3: Box plot of the NRMSD for all 7 SNR classes and different reconstruction algorithms outlined in the figure label.
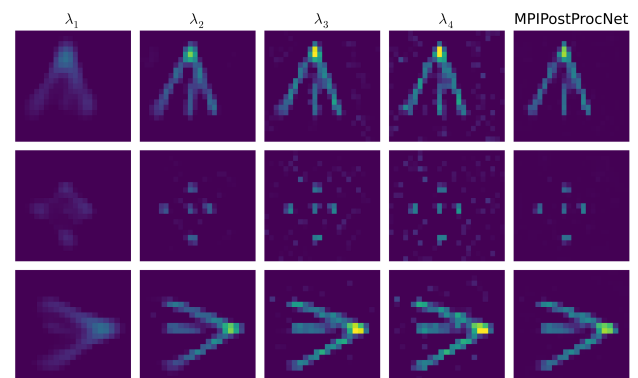

Figure 4: Central slices (1st row: yz, 2nd row xz, 3rd row xy) of the resolution phantom of the OpenMPIData set. First four columns show the pre-reconstructions while the fifth column shows the result of MPIPostProcNet.

truth is available. The MPIPostProcNet yields a better result than this idealized case.

Reconstruction results for resolution phantom of the OpenMPIData are shown in Figure 4. The neural network successfully removes the noise present in the pre-reconstructions while preserving the full resolution of the reconstructions obtained for λ_3 and λ_4.

IV. Conclusion and Discussion

In summary, we have developed a novel neural network-based post-processing method for improved image reconstruction in magnetic particle imaging. Our main goal was to develop an automatic reconstruction algorithm that does not require manual fine-tuning of regularization parameters. We achieved this by performing reconstruction with different regularization parameters and combining the results with a data-driven learning approach. Our results show that the proposed MPIPostProcNet indeed yields very good results, both qualitatively and quantitatively. Compared to the best pre-reconstruction, the results are even better for all SNR values.

For the robustnes of the method, it is important that any of the regularization parameters used for pre-reconstruction are somewhat close to the optimal regularization parameter. Robustness could thus be further increased by increasing the number of pre-reconstructions. One drawback of our approach is the increase in reconstruction time, which scales proportionally with the number of pre-reconstructions L. However, since the Kaczmarz reconstruction used is quite fast and a small number of $L = 4$ is sufficient in our experiments, the increase in computation time should be acceptable when using a suitable multi-threaded implementation.

A characteristc of MPIProcNet is the simple architecture, which can be easily integrated with existing MPI reconstruction pipelines. Moreover, it would be easy to adapt the method to different, potentially more sophisticated pre-reconstruction methods. Finally, comparing the network output to the pre-reconstructions allows one to easily control the plausibility of the network output, which makes it easy to develop trust in MPIProcNet.

Author's statement

Conflict of interest: Authors state no conflict of interest.

References

[1] T. Knopp, S. Biederer, T. Sattel, and T. M. Buzug, Singular value analysis for magnetic particle imaging, in *2008 IEEE Nuclear Science Symposium Conference Record*, IEEE, 4525–4529, 2008.

[2] P. Koch, M. Maass, M. Bruhns, C. Droigk, T. J. Parbs, and A. Mertins, Neural network for reconstruction of MPI images, in *International Workshop on Magnetic Particle Imaging*, 39–40, 2019.

[3] A. von Gladiss, I. Kramer, N. Theisen, R. Memmesheimer, A. C. Bakenecker, T. M. Buzug, and D. Paulus. Data augmentation for training a neural network for image reconstruction in MPI. *International Journal on Magnetic Particle Imaging*, 8(1 Suppl 1), 2022.

[4] B. Askin, A. Güngör, D. Alptekin Soydan, E. U. Saritas, C. B. Top, and T. Cukur, PP-MPI: A deep plug-and-play prior for magnetic particle imaging reconstruction, in *International Workshop on Machine Learning for Medical Image Reconstruction*, Springer, 105–114, 2022.

[5] S. Dittmer, T. Kluth, M. T. R. Henriksen, and P. Maass. Deep image prior for 3D magnetic particle imaging: A quantitative comparison of regularization techniques on Open MPI dataset. *International Journal on Magnetic Particle Imaging*, 7(1), 2021.

[6] T. Knopp and M. Grosser, Warmstart approach for accelerating deep image prior reconstruction in dynamic tomography, in *Medical Imaging with Deep Learning*, PMLR, 2022.

[7] T. Knopp, J. Rahmer, T. F. Sattel, S. Biederer, J. Weizenecker, B. Gleich, J. Borgert, and T. M. Buzug. Weighted iterative reconstruction for magnetic particle imaging. *Physics in Medicine and Biology*, 55(6):1577, 2010.

[8] T. Knopp, P. Szwargulski, F. Griese, and M. Gräser. OpenMPIData: An initiative for freely accessible magnetic particle imaging data. *Data in Brief*, 28:104971, 2020.

[9] O. Ronneberger, P. Fischer, and T. Brox, U-net: Convolutional networks for biomedical image segmentation, in *International Conference on Medical image computing and computer-assisted intervention*, Springer, 234–241, 2015.

[10] K. Zhang, W. Zuo, Y. Chen, D. Meng, and L. Zhang. Beyond a gaussian denoiser: Residual learning of deep cnn for image denoising. *IEEE Transactions on Image Processing*, 26(7):3142–3155, 2017.